Eur. Phys. J. B **9**, 613–618 (1999)

THE EUROPEAN PHYSICAL JOURNAL B

EDP Sciences

Magnetic interactions in the monoclinic ludwigite $Cu_2FeO_2BO_3$

M.A. Continentino[1,a], J.C. Fernandes[1], R.B. Guimarães[1], H.A. Borges[2], A. Sulpice[3], J-L. Tholence[4], J.L. Siqueira[5], J.B.M. da Cunha[5], and C.A. dos Santos[5]

[1] Instituto de Física, Universidade Federal Fluminense, Campus da Praia Vermelha, Niterói, 24210-340, RJ, Brazil
[2] Departamento de Física, Pontifícia Universidade Católica do Rio de Janeiro, Rio de Janeiro, 22452-970, RJ, Brazil
[3] Centre de Recherches sur les Très Basses Temperatures-CNRS, 25 avenue des Martyrs, BP 166, 38042 Grenoble Cedex 9, France
[4] Laboratoire des Propriétés Électroniques des Solides-CNRS, 25 avenue des Martyrs, BP 166, 38042 Grenoble Cedex 9, France
[5] Instituto de Física, Universidade Federal do Rio Grande do Sul, avenue Bento Gonçalves, 9500, Porto Alegre, 91501-970, RS, Brazil

Received 25 September 1998

Abstract. The system $Cu_2FeO_2BO_3$ is an oxyborate belonging to the family of the ludwigites. In this paper we present AC susceptibility, magnetization measurements and Mössbauer spectroscopy on this material which allows for a complete characterization of its complex magnetic behavior. We find an hierarchy of interactions which clearly defines three regimes with decreasing temperature. These are associated with, the freezing of the Fe moments, the antiferromagnetic ordering of the Cu sub-lattice and finally the coupling between both systems.

PACS. 75.30.Cr Saturation moments and magnetic susceptibilities – 75.10.Nr Spin-glass and other random models – 75.60.Ej Magnetization curves, hysteresis, Barkhausen and related effects – 76.80.+y Mössbauer effect; other γ-ray spectroscopy

1 Introduction

The ludwigites belong to the family of oxyborates which includes compounds having several chemical compositions and *circa* ten known different crystalline structures. One of the main intriguing problems related to the oxyborates is to understand how the low dimensionality they present, determines their magnetic and electric behavior. For the purpose of understanding such inter-relation we carried out a detailed study on several magnetic warwickites which constitute another well known structure of the oxyborate family [1–3]. The structure of these systems can be viewed as an assembling of sub-units, in the form of ribbons, where the magnetic ions are randomly located. Consequently, disorder and low dimensionality are the basic ingredients underlying the magnetic and electric properties of these materials. They give rise to localization and typical random exchange Heisenberg antiferromagnetic chain (REHAC) behavior. More recently we have extended our investigations to the ludwigites, specifically the system $Ni_2FeO_2BO_3$, which instead of ribbons show zig-zag walls with metallic ions [4] (see Fig. 1 of Ref. [4]).

The general chemical formula of ludwigites is $M_2^{2+}M^{3+}O_2BO_3$ where M^{2+} or M^{3+} or both are $3d$ transition metals. All the crystalline structures of oxyborates are quite similar: the divalent and trivalent metals, respectively M^{2+} and M^{3+}, are found at the centers of edge-sharing oxygen coordination octahedra which form ribbons in warwickites and zig-zag walls in ludwigites. The boron ions remain at the centers of oxygen coordination triangles, each corner of which is a corner of a different octahedra. The trigonal borate groups BO_3^{3-} are the strongest bonded groups of ions in the oxyborates and are responsible for the bonding between ribbons or walls. The oxyborates present also atomic positional disorder since the metals M^{2+} and M^{3+} may occupy any of the distinct metal crystalline sites. These are two for warwickites and four for ludwigites. The association of low-dimensionality and disorder is then a common feature of oxyborates. The occupancy of each site does not change significantly with chemical composition for each crystalline structure.

The crystalline structure of the ludwigites is orthorhombic with space group *Pbam*. However, the copper ludwigites, one of which is the object of this study, present a monoclinically distorted variant of this structure with space group $P2_1/c$ due to a strong Jahn-Teller effect [5]. A detailed description of the ludwigite structure may be found in the references given in Table 1. This table gives the chemical formulae of the ludwigites whose crystalline structures have been refined after X-ray measurements. Available magnetic parameters are also shown.

[a] e-mail: mucio@if.uff.br

Table 1. Chemical formulae, references on crystalline refinements, magnetic ordering or coupling temperatures and references on magnetic measurements of ludwigites. A: references on crystalline refinements; B: references on magnetic properties; (*): present paper; other symbols defined in the text.

Chemical formula	A	T_f	$T_{N^{Ni,Cu}}$	T_N	B
$Mg_2MnO_2BO_3$	[6]				
$Mg_2FeO_2BO_3$	[7]	10 K			[8]
$Fe_2^{2+}Fe^{3+}O_2BO_3$	[9]			98 K	[9]
$Co_2^{2+}Co^{3+}O_2BO_3$	[6]				
$Co_{2.1}Al_{0.9}O_2BO_3$	[5]				
$Ni_2VO_2BO_3$	[10]				
$Ni_2CrO_2BO_3$	[10]				
$Ni_2FeO_2BO_3$	[11]	106 K	46 K	15 K	[4]
$Ni_2AlO_2BO_3$	[5]				
$Cu_2AlO_2BO_3$	[5]				
$Cu_2FeO_2BO_3$	[12]	63 K	38 K	20 K	*

This paper reports AC magnetic susceptibility, magnetization and Mössbauer spectroscopy studies in the ludwigite $Cu_2FeO_2BO_3$. For susceptibility measurements an ensemble of oriented monocrystalline needles has been employed (about 4 mm long). The other measurements have been carried out in powder samples. Also, the X-ray identification of the crystalline structure is presented. The results of our magnetic measurements in this compound have some distinct features compared to those we have obtained for $Ni_2FeO_2BO_3$ [4]. This is due to the monoclinic distortion presented by the copper ludwigites which gives rise to a stronger magnetic anisotropy. Our results indicate that the Fe^{3+} ($S = 5/2$) and Cu^{2+} ($S = 1/2$) subsystems behave as two decoupled magnetic systems of spins down to approximately 20 K in the absence of an external magnetic field. The coupling temperature is lowered if a magnetic field is applied. Such a dependence on applied field has not been observed in the nickel ludwigite since the low temperature peak in the isothermal curves M/H *vs.* H was less pronounced. Within the Cu and Fe subsystems the coupling is essentially antiferromagnetic-like and due to superexchange. This is consistent with the fact that there is no evidence of macroscopic magnetization. The 3D ordering of the iron and copper subsystems occur at 63 K and 38 K respectively. The former transition is now clearly visible in the AC susceptibility. This was not the case in $Ni_2FeO_2BO_3$ due to the larger susceptibility of Ni, compared to that of Cu, which obscured the Fe contribution. For the more dilute Fe subsystem the ordering at 63 K is of the spin-glass type as in most dilute random magnetic system with antiferromagnetic couplings. This is also the case for the ludwigite $Mg_2FeO_2BO_3$ where Fe is the only magnetic component [8].

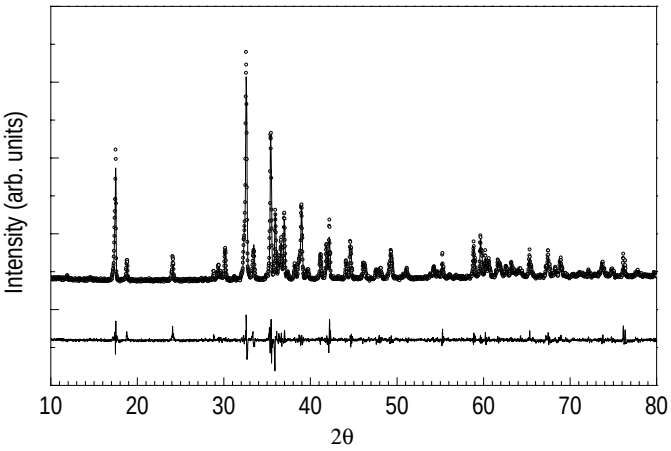

Fig. 1. Room temperature X-ray powder diffraction pattern for the ludwigite $Cu_2FeO_2BO_3$. The open circles represent the observed data. The solid line represents the calculated pattern obtained from the Rietveld refinement. The lower trace is a plot of the residual spectrum, *i.e.*, the difference between experimental, calculated intensities.

2 Sample preparation and characterization

The sample was synthesized from stoichiometric mixture of the oxides CuO and Fe_2O_3 in borax. The mixture was heated at 950 °C in pure oxygen atmosphere during two days and, then slowly cooled. Blue dark needles were obtained reaching 4 mm in length.

X-ray powder diffraction (XRPD) patterns were obtained in Bragg-Brentano geometry by means of a Siemens diffractometer D5000 equipped with a curved graphite monochromator and CuKα radiation ($\lambda = 1.5418$ Å). Measurements were performed with a scan step of 0.02° in the 2θ range from 5° to 100° with a fixed counting time of 4s. The program Fullprof [13] was used for structure indexing and cell parameters calculation. The XRPD pattern, shown in Figure 1, was indexed to the space group $P2_1/c$ with unit cell parameters comparable to those previously reported for a similar sample [12]. The good quality of the sample, without signs of spurious phases, is verified by the small intensities of the residual spectrum also shown in Figure 1.

3 Measurements

3.1 Magnetic susceptibility

The real part of the AC susceptibility of $Cu_2FeO_2BO_3$, χ_{ac},was measured at 125 Hz in a Lake-Shore apparatus. Figure 2 shows the temperature dependence of $1/\chi_{ac}(T)$. The paramagnetic Curie temperature $\theta_N = -178$ K indicates strong antiferromagnetic couplings. In spite that the Cu spins are in majority this high temperature Curie Weiss term is dominated by the Fe spins due to their larger magnetic moment ($\theta_N \propto S(S+1)$). Also the Fe sub-system orders at higher temperatures than the Cu one. This ordering is characterized by the small anomaly

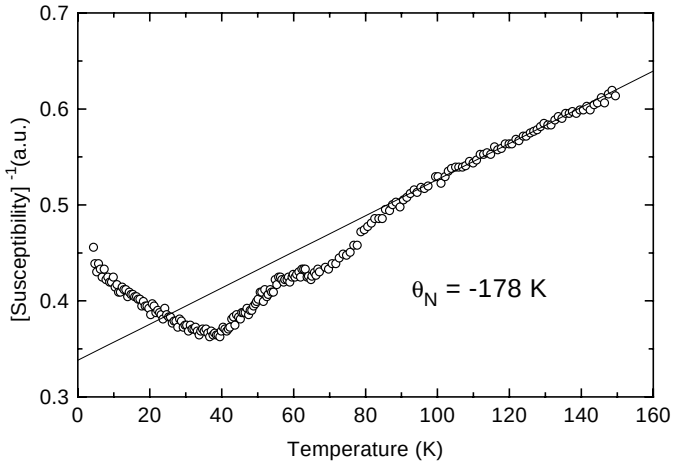

Fig. 2. Inverse AC magnetic susceptibility of $Cu_2FeO_2BO_3$, χ_{ac}, measured at 125 Hz under an oscillating applied field of 10 Oe.

in the χ_{ac} susceptibility at $T_f^{Fe} \approx 63$ K and is associated with a spin glass freezing of the Fe component. This is confirmed by the Mössbauer experiments discussed further on. Below this temperature, the susceptibility is essentially due to the Cu spins which in turn order antiferromagnetically at $T_N^{Cu} \approx 38$ K, as evidenced by the intense peak in the susceptibility at this temperature. It is interesting to compare the present results with the previously studied $Ni_2FeO_2BO_3$ system [4]. We found there, that the majority Ni component of this ludwigite orders at $T_N^{Ni} \approx$ 46 K and we attribute the larger ordering temperature in this case, than in the Copper case, to the larger Ni spin ($S = 1$).

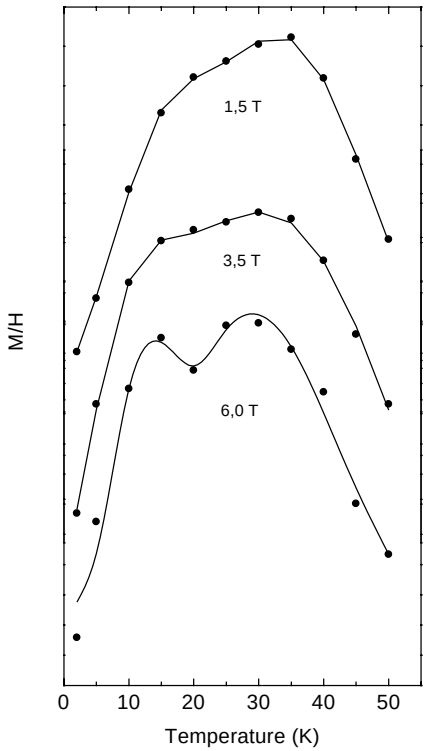

Fig. 3. Magnetic susceptibility (M/H) *vs.* temperature curves for the ludwigite $Cu_2FeO_2BO_3$ obtained from the isothermal magnetization curves for three values of the applied magnetic field. The continuous lines are the actual fits of these results using two Lorentzians. The temperature of the maxima of the Lorentzians for several fields are shown in Figure 4. The error in each experimental points is less than 1/1000 of the (M/H) value.

3.2 Magnetization

Magnetic measurements were performed using a superconducting quantum interference device magnetometer in the temperature range from 4 K to 50 K and in fields from $H = 0$ to $H = 7.5$ T. We have measured the magnetization M as a function of field H for different fixed temperatures. From these isotherms we have obtained M/H *vs.* T curves for different applied magnetic fields H. Some of these curves are shown in Figure 3. The M/H *vs.* T curves can be fitted using two Lorentzians, as shown in Figure 3, which for $H = 1.5$ T, peak at T_N^{Cu} =35.7 K and $T_N = 14.4$ K respectively. Both peaks shift to lower temperatures, as the applied magnetic field increases, making evident this two peak structure of the M/H *vs.* T curves. Further support for this analysis comes from our previous experience with $Ni_2FeO_2BO_3$ where the lower temperature peak, also appears as a small anomaly in χ_{ac}. This low temperature peak is associated with the coupling between the two magnetic subsystems, in the present case the Fe and Cu subsystems. In Figure 4 we show the temperatures of the peaks in the susceptibility, (M/H), as functions of the external magnetic field. The high temperature peak clearly marks the AF ordering of the Cu subsystem, as it extrapolates smoothly to the Neel temperature in zero field obtained in the AC susceptibility measurements. This peak shifts to lower temperatures on the application of an external magnetic field as expected for an antiferromagnetic transition. This shift is very much reduced when compared to that of T_{Ni}^N in $Ni_2FeO_2BO_3$. This is due to the strong anisotropy which arises from the Jahn-Teller nature of the Cu^{2+} ion. Notice that the low temperature peak, for $H = 0$, extrapolates to $T_N(H = 0) \approx 20$ K a temperature for which the Mössbauer spectra has qualitative changes, as discussed below. These results taken together provide strong support for our analysis of the (M/H) curves and the interpretation of the coupling temperatures.

Curves of M *vs.* T for two different histories, field cooled (FC) and zero-field cooled (ZFC) ($H = 3$ T), are shown in Figure 5 and present irreversibility or history dependent effects starting below $T_N^{Cu}(H)$ which is due to the spin glass component associated with the Fe sublattice. The magnetization curve obtained at 4 K is shown in Figure 6. It does not show any significant hysteresis or remanent magnetization near $H = 0$ indicating antiferromagnetic coupling *within each subsystem.*

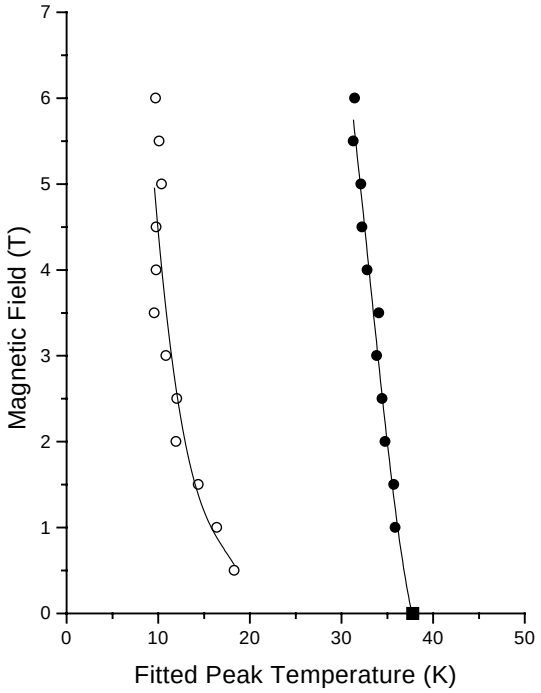

Fig. 4. Temperatures of the peaks of the Lorentzians used to fit the (M/H) curves *vs.* applied field for $Cu_2FeO_2BO_3$ and which represent the Neel temperature of the Cu sublattice $T_N^{Cu}(H)$ and the coupling of the subsystems $T_N(H)$.

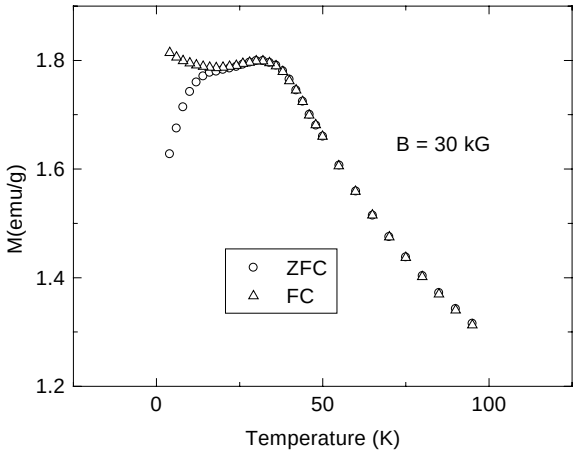

Fig. 5. Magnetization *vs.* temperature curve, under an applied field of 30 kG, for $Cu_2FeO_2BO_3$. The splitting is due to FC and ZFC regimes.

3.3 Mössbauer spectroscopy

MS measurements were performed between 4.2 K and 300 K. The spectra were taken using a constant acceleration electromechanical drive system with a multichannel analyzer for collecting and storing the data. The temperature stability was better than 0.1 K. ^{57}Co in rhodium was used at room temperature as source, with nominal activity of 20 mCi. The hyperfine parameters for the paramagnetic spectra were obtained by a least-squares procedure assuming Lorentzian line shapes constrained to equal

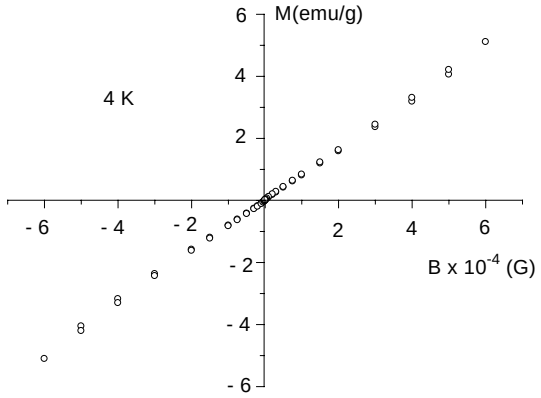

Fig. 6. Magnetization *vs.* applied field curve for $Cu_2FeO_2BO_3$ at 4 K showing the very small hysteresis and remanent magnetization of the system.

Table 2. Hyperfine parameters for $Cu_2FeO_2BO_3$ measured at 300 K. ΔE_Q is the quadrupole splitting at the iron sites; δ_{Fe} is the isomer shift relative to α-Fe; Γ is the linewidth at half-height; A is the site occupancy, given by the relative spectral area. Typical errors are $\pm 3\%$ on hyperfine parameters and $\pm 5\%$ on site occupancies.

ΔE_Q (mm/s)	δ_{Fe} (mm/s)	Γ (mm/s)	A (%)	Site assignment
0.50	0.34	0.27	10	1
0.68	0.34	0.27	20	2
0.98	0.33	0.46	70	3,4

halfwidths. Following the Window model, the spectra obtained in the magnetically ordered regime were fitted to a hyperfine field distribution (HFD), $p(H)$, by superposing subspectra with Lorentzian lineshapes, constrained to equal quadrupole splitting, isomer shift and halfwidths. Typical errors are $\pm 3\%$ on hyperfine parameters and $\pm 5\%$ on site occupancies.

From room temperature (RT) to about 60 K the sample is in the paramagnetic regime, represented by three symmetrical doublets (see Fig. 7), whose hyperfine parameters for $T = 300$ K are displayed in Table 2.

All the doublets could be fitted to isomer shift values relative to αFe smaller than 0.4 mm/s, characteristic of Fe^{3+}. However, some of the fitted quadrupole splittings could be attributed to both Fe^{2+} or high spin Fe^{3+}. We attributed the three doublets to high spin Fe^{3+} since the isomer shift is more sensitive to the oxidation state than the quadrupole splitting. Such a behavior has been observed in $RbFeF_4$ and $KFeF_4$ [14] as well as in $Ni_2FeO_2BO_3$ [4]. However, the Fe^{3+} character is best defined here than for $Ni_2FeO_2BO_3$. The site assignment displayed in Table 2 was based on the structural refinement. As compared to those obtained for $Ni_2FeO_2BO_3$ [4], it is interesting to point out that all the tentative to fit the present RT spectrum to four doublets were unsuccessful. Furthermore, we have not here a large doublet corresponding to the site 4, as assigned for $Ni_2FeO_2BO_3$ [4]. We have attributed

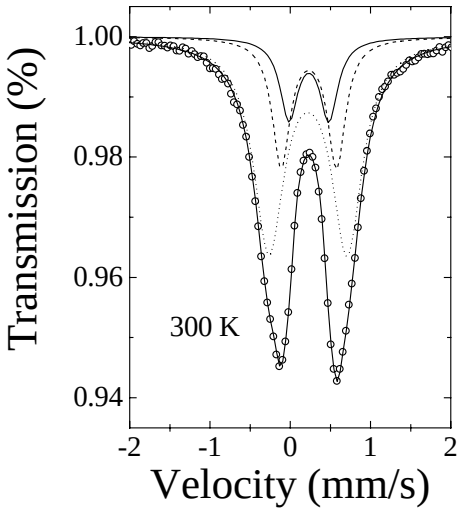

Fig. 7. Mössbauer spectrum from $Cu_2FeO_2BO_3$ (circles) at $T = 300$ K. The continuous curves represent the fitted spectra for each one of the four crystallographic Fe sites.

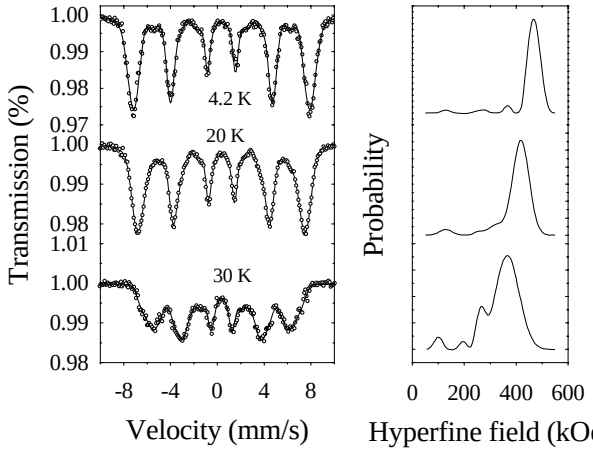

Fig. 8. Mössbauer spectra from $Cu_2FeO_2BO_3$ taken at different temperatures below T_N^{Cu} and the hyperfine field distributions for the spectra shown.

Table 3. Hyperfine parameters for $Cu_2FeO_2BO_3$ measured at low temperatures. ΔE_Q is the quadrupole splitting at the iron sites; δ_{Fe} is the isomer shift relative to α-Fe; Γ is the linewidth at half-height for all the Lorentzian used in the fitting; H_0 is the hyperfine field for isolated ^{57}Fe; H_1, H_2 and H_3 are attributed to iron atoms with different exchange interactions; A_i is the relative area corresponding to the contribution of the hyperfine field H_i to the total spectrum.

	30 K	20 K	4.2 K
H_0 (kOe)	100	129	129
A_0(%)	8	4	2
H_1 (kOe)	195	253	268
A_1(%)	4	2	3
H_2 (kOe)	265	323	366
A_2(%)	12	4	9
H_3 (kOe)	366	418	468
A_3(%)	76	85	91
ΔE_Q (mm/s)	-0.02	-0.01	-0.01
δ_{Fe}(mm/s)	0.47	0.47	0.47
Γ (mm/s)	0.57	0.54	0.54

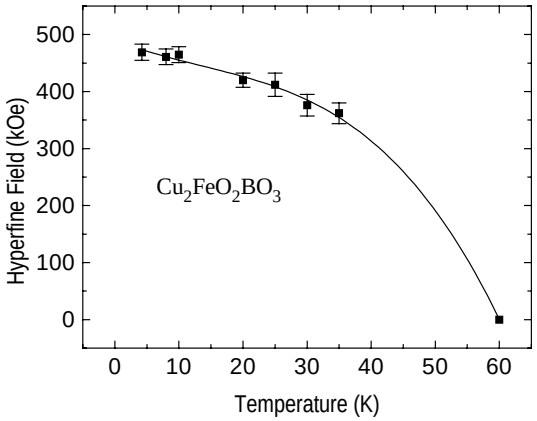

Fig. 9. Iron hyperfine fields *vs.* temperatures for $Cu_2FeO_2BO_3$ (circles). The curve is a guide to the eyes.

the large halfwidths of the doublet with 0.98 mm/s as an indication of the superposition of two doublets. Therefore, as indicated in Table 2, this doublet was assigned to sites 3 and 4.

The spectrum taken at 60 K is very similar to that obtained at 300 K. However, an accurate examination showed that relaxation effects are present at this temperature. As the temperature decreases below 60 K, a noticeable broadening of the peaks is clearly observed, emphasizing the relaxation effects. From 60 K down to about 20 K, the system is within a slowing down process toward the saturated state. These results clearly indicate a spin glass freezing of the Fe moments below 60 K down to 20 K where this subsystem couples to that of Cu moments. This intermediate regime will be fully reported elsewhere. The spectrum taken at 30 K (see Fig. 8) is typical of this temperature range. All the spectra taken below 30 K were fitted with four hfd components centered at fields displayed in Table 3.

As for the warwickite $MgFeOBO_3$ [2] the distribution centered at about 100 KOe is attributed to decoupled iron. This contribution is present even at low temperatures such as 4.2 K (Fig. 8). In fact, the Mössbauer spectra obtained below 20 K are quite similar and all of them indicate that the system is nearly saturated, with the most probably hyperfine field larger than 400 kOe and small contribution from the other distributions (see Tab. 3). The most probable hyperfine field as a function of temperature is shown in Figure 9. It is interesting to note the consistent temperature dependence of the hyperfine parameters as compared to that observed for $Ni_2FeO_2BO_3$ [4]. The isomer shift changes from about 0.30 mm/s at RT to 0.47 mm/s at 4.2 K, while the quadrupole splitting is virtually zero in the ordered regime. Concerning the temperature

dependence of the quadrupole splitting, such a behavior has been observed in other disordered systems and early discussed by Ridout [15].

4 Discussion

Our magnetic studies of the ludwigite system $Cu_2FeO_2BO_3$ has revealed the existence of three anomalies in the behavior of this material which can be unequivocally identified. The first at $T_f^{Fe} = 63$ K can be easily associated with the spin glass freezing of the Fe sub-lattice since this is the temperature below which the Zeeman splitting in the Mössbauer spectra appears. The AC susceptibility has an anomaly at this temperature. At $T_N^{Cu} = 38$ K, the Cu subsystem orders antiferromagnetically, as shown by an intense peak in the AC susceptibility. There is no evidence of such ordering in the Mössbauer experiments indicating that down to this temperature both magnetic subsystems are decoupled of each other. This is consistent with Goodenough rules [16] for cation-cation magnetic interactions in oxides. Such rules predict a negligible value for the direct interaction between Cu^{2+} and Fe^{3+} if their coordination octahedra share a face or an edge as is the case in the ludwigites. Finally at $T_N(H = 0) \approx 20$ K both systems couple magnetically. This coupling shows up in the susceptibility (M/H) curves and also in the Mössbauer experiments. Magnetization curves at 4.2 K show negligible hysteresis and remanent magnetization. It is interesting that the cancelation of the total magnetization takes place *within each subsystem*, in agreement with the fact that they order magnetically independently of each order. We have found that both T_N^{Cu} and T_N shift to lower values in an applied magnetic field. However the shift of the Cu antiferromagnetic ordering temperature is much smaller than that of Ni in $Ni_2FeO_2BO_3$. This is due to the strong anisotropy which arises from the monoclinic distortion of the Cu ludwigite. Notice also that in spite of the smaller value of the Cu spin, as compared to that of Ni, there is only a small reduction of the ordering temperature since this is compensated by the magnetic anisotropy due to the Jahn-Teller distortion. The low dimensionality of the system, constituted of zig-zag walls, manifests in a discrepancy between the large paramagnetic Curie temperature, which indicates strong antiferromagnetic interactions and the much reduced ordering temperature of the Fe moments. In the present system the ordering temperatures are too close to allow for a meaningful analysis of the temperature dependence of the susceptibility in terms of a non trivial power law, which is indicative of random exchange Heisenberg antiferromagnetic chain behavior [4]. This would be expected since there are sites along the walls with occupancies as high as, say 73% Fe. These *lines* of Fe isolate the Cu chains along the walls giving rise to pseudo one-dimensional behavior before the 3d crossover.

We would like to thank CNPq, FAPERJ and FINEP for partial financial support.

References

1. J.C. Fernandes, R.B. Guimarães, M.A. Continentino, H.A. Borges, J.V. Valarelli, A. Lacerda, Phys. Rev. B **50**, 16754 (1994).
2. R.B. Guimarães, J.C. Fernandes, M.A. Continentino, H.A. Borges, C.S. Moura, J.B.M. da Cunha, C.A. dos Santos, Phys. Rev. B **56**, 292 (1997).
3. J. Dumas, M.A. Continentino, J.J. Capponi, J-L. Tholence, Solid State Commun. **106**, 35 (1998).
4. J.C. Fernandes, R.B. Guimarães, M.A. Continentino, H.A. Borges, A. Sulpice, J-L. Tholence, J.L. Siquiera, L.I. Zawislak, J.B.M. da Cunha, C.A. dos Santos, Phys. Rev. B **58**, 287 (1998).
5. J.A. Hriljac, R.D. Brown, A.K. Cheetham, J. Solid State Chem. **84**, 289 (1990).
6. R. Norrestam, K. Nielsen, I. Sotofte, N. Thorup, Z. Kristall. **189**, 33 (1989).
7. Y. Takeuchi, T. Watanabe, T. Ito, Acta Cryst. **3**, 98 (1950).
8. H. Neuendorf, W. Gunßer, J. Magn. Magn. Mater. **173**, 117 (1997).
9. J.S. Swinnea, H. Steinfink, Am. Mineral. **68**, 827 (1983).
10. R. Norrestam, M. Kritikos, K. Nielsen, I. Sotofte, N. Thorup, J. Solid State Chem. **111**, 217 (1994).
11. S.A. DeWaal, E.A.Viljoen, L.C.Calk, Trans. Geol. Soc. S. Afr. **77**, 375 (1974).
12. JCPDS-ICDD file 31-460 (1992).
13. J. Rodriguez-Carvajal, *Short reference guide of the program FULLPROF* (1997). Version 3.2 available in `pub/divers/fullp` of the anonymous ftp area of the LLB unix cluster.
14. H. Keller, I. Savić, Phys. Rev. B **28**, 2638 (1983).
15. M.S. Ridout, J. Phys. C 2, 1258 (1969).
16. J.B. Goodenough, Phys. Rev. **117**, 1442, (1960).